Spectral Consequences of Broken Phase Coherence in $1T$-TaS_2

F. Zwick,[1] H. Berger,[1] I. Vobornik,[1] G. Margaritondo,[1] L. Forró,[2] C. Beeli,[3] M. Onellion,[4] G. Panaccione,[5] A. Taleb-Ibrahimi,[5] and M. Grioni[1]

[1]*Institut de Physique Appliquée, Ecole Polytechnique Fédérale, CH-1015 Lausanne, Switzerland*
[2]*Laboratoire de Physique des Solides Semicristallins, IGA, Ecole Polytechnique Fédérale, CH-1015 Lausanne, Switzerland*
[3]*CIME, Ecole Polytechnique Fédérale, CH-1015 Lausanne, Switzerland*
[4]*Department of Physics, University of Wisconsin, Madison, Wisconsin 53706*
[5]*LURE, Université Paris-Sud, 91405 Orsay, France*
(Received 22 January 1998)

Random defects destroy long-range phase coherence, and inhibit the metal-insulator transition in the charge density wave (CDW) system $1T$-TaS_2. Photoelectron spectroscopy with high resolution reveals corresponding changes in the electronic structure. Core level spectra indicate a temperature-dependent limited growth of commensurate CDW domains. Screening by free carriers from the domain boundaries reduces the Coulomb repulsion in the Ta d band by $\sim 1/3$, compared to pure samples, yielding a finite spectral weight at the Fermi level. [S0031-9007(98)06833-1]

PACS numbers: 71.30.+h, 71.45.Lr, 73.20.Dx, 79.60.Bm

Metal-insulator (MI) transitions in two-dimensional systems of correlated fermions are a subject of continuing interest. Quasi-two-dimensional (quasi-2D) materials, like the layered transition metal dichalcogenides, which exhibit broken symmetry ground states [1], can help us understand the emergence of long range order in systems dominated by strong local interactions. We present here results on $1T$-TaS_2, a 2D system which offers a fascinating example of MI transition, where local interactions, long-range charge order, and defects are all important and interrelated.

$1T$-TaS_2 presents a modulation of the electronic density, or charge density wave (CDW) which, depending on temperature, is incommensurate (IC), nearly commensurate (NC), or commensurate (C), with the underlying lattice [1]. In the NC phase, stable at room temperature, the CDW forms a hexagonal array of commensurate domains with typical size of 60 Å. The domains are separated by domain walls, or discommensurations, where the CDW phase changes rapidly [2–4]. At lower temperature the CDW locks-in to the lattice via a first order transition to a commensurate (C) $\sqrt{13}x\sqrt{13}$ phase. At the transition, the in-plane resistivity increases by 1 order of magnitude, and the whole Fermi surface is disrupted [5]. This major rearrangement of the electronic structure is now understood as a Mott-Hubbard localization, triggered by the NC-C transition [6].

Experiments on alloys [7] and on irradiated samples [8], as well as theoretical considerations [9], indicate that disorder has a strong influence on the properties of $1T$-TaS_2. Defects and impurities act as pinning centers for the CDW [10], and failure to establish long-range order inhibits the NC-C and Mott-Hubbard transitions. But what is the effect on the electronic structure? We addressed this question by high-resolution photoelectron spectroscopy, comparing pure samples of $1T$-TaS_2 with samples where the MI transition had been suppressed by defects. We find spectroscopic evidences that defects limit the size of the CDW domains in the NC phase. More importantly, we find that disorder modifies the electronic states near the Fermi surface. Valence band spectra indicate that the electron-electron Coulomb interaction strength is reduced by $\sim 1/3$ in the disordered material. The system is frozen short of a Mott-Hubbard transition, and the spectral weight at the chemical potential remains finite at all temperatures.

$1T$-TaS_2 single crystals were grown in fused silica ampoules by halogen chemical-vapor transport, from high-purity Ta wire (Alpha 99.997%) and vacuum-resublimed sulfur (Atomenergic 99.9999%). We used ICl_3 as transport agent, and a gradient of 7OO-65O C. Crystals grow as yellow-metallic platelets in the cooler zone of the furnace, in 10–14 days. The crystals obtained by this procedure, which does not require quenching from high temperature [11], exhibit the 1T polytype, and are considerably thicker (up to 2 mm) than those obtained by using iodine as a transport agent. They present a clear first order NC-C transition at 160 K, with a characteristic hysteresis. By using less pure Ta (Alpha 99.98%-Niobium 5O ppm), and the same nominal growth conditions, we obtained 1T samples (hereafter disordered-TaS_2 or d-TaS_2) which did not exhibit the NC-C transition [11]. The stoichiometries of the two kinds of samples, measured by microprobe analysis, were identical within the sensitivity of the technique <1000 ppm.

We performed high-resolution core level and angle-resolved (ARPES) photoemission measurements at the Franco-Swiss SU3 undulator beam line of the Super-Aco storage ring, in Orsay, and at the Wisconsin Synchrotron Radiation Center. The samples were cleaved at a base pressure of 1×10^{-10} torr, and their temperature could be varied between RT and 85 K. We used low-energy electron diffraction (LEED) to verify the sample orientation, and the CDW superstructure. Photoelectrons

 0031-9007/98/81(5)/1058(4)$15.00 © 1998 The American Physical Society

were analyzed by a 150 mm mean-radius hemispherical electrostatic analyzer. The total energy resolution (electrons + photons) was 60 meV for the core level and 30 meV for the valence band spectra, and the angular resolution was $\Delta\theta = 2°$.

Figure 1 compares the in-plane resistivity of representative TaS_2 and d-TaS_2 crystals. The data for the pure sample are consistent with the literature [5]. The jump at the NC-C transition is entirely suppressed in d-TaS_2, and the resistivity is that of a disordered semimetal. The RT value is close to that of the pure sample, but large differences are observed at low temperature, in close analogy with data on doped or irradiated samples [7,8].

Transmission electron microscopy (TEM) measurements on very thin flakes cleaved from the same crystals show corresponding differences in the structure and morphology of the two samples. We collected selected area electron diffraction (SAED) patterns between 390 and 120 K. We observed sharp IC-NC (at ~350 K) and NC-C transitions in pure TaS_2. The disordered sample, on the other hand, showed only a gradual transition from the IC to the NC phase, and the SAED pattern of the NC was still visible at 120 K, indicating a lower degree of phase coherence in d-TaS_2. The bright field images of Fig. 2 suggest a possible cause for these differences. Both crystals show an extended dislocation network with rather straight dislocations, separated by several 10 μm, which we attribute to deformations induced by the TEM sample preparation. In d-TaS_2, however, additional intrinsic defects appear as slightly wavy or bent weaker contrast lines, with a typical separation of 0.2 to 0.5 μm. Similar defect structures are absent from pure TaS_2. The data indicate that these additional defects may stabilize the NC phase in d-TaS_2, preventing the metal-insulator transition.

Previous ARPES experiments have shown that the NC-C transition is accompanied by characteristic changes of the electronic structure near the Fermi surface [12–15]. Our data on the pure sample are consistent with those results. The intensity plots of Fig. 3, obtained from the raw ARPES data, outline the electronic bands along the high-symmetry ΓM direction. In the NC phase, the Ta $d_{3z^2-r^2}$ band [13] disperses upwards from the M point and crosses the Fermi level at $\sim 1/3$ of the ΓM distance. Weakly dispersing states also appear near E_F around the Γ point. The observed blurring of the band can be attributed to the finite domain size. In the C phase, under the influence of the CDW potential, the band splits into three subbands [6,13], which can be identified in the intensity plot. According to the model of Tosatti and Fazekas (TF), electronic correlations further split the half filled narrow subband straddling the Fermi level, and yield an insulating ground state. The flat lower Hubbard band (LHB), is well visible around Γ at a binding energy of 0.19 eV [16].

The MI transition is closely linked to the growth of the C domains, in the NC phase, as temperature is reduced. Core level spectra provide information on the domain size, complementary to structural techniques [3]. The Ta $4f$ binding energy is sensitive to the local charge density at Ta sites, which is modulated by the CDW [12,17–19]. In the IC phase ($T > 350$ K), all Ta sites are inequivalent, and the spectral line shape is simply broadened. The C phase has only three inequivalent Ta sites, with occupation 6:6:1, and the $4f$ levels are split into well separated sublevels (only two are readily identified). In the intermediate NC phase, the splitting is incomplete, reflecting the relative size of the commensurate domains and domain boundaries. In Fig. 4, the progressive splitting of the Ta $4f_{7/2}$ line in the pure sample (and of its spin-orbit partner, not shown), follows the domain growth. Because of the large hysteresis of the transition [5], the spectrum measured at 190 K upon cooling or heating from the C phase do not coincide.

The 300 and 190 K Ta $4f$ spectra of the disordered sample are identical to those of TaS_2, suggesting similar domain sizes in the two samples. The splitting increases at lower temperature, but it remains incomplete even at 90 K, indicating the absence of long-range order. Spectra measured at 190 K upon cooling and upon heating are now identical, since the hysteresis has disappeared with the lock-in transition.

The main result of our investigation of the influence of disorder on the MI transition is illustrated by the valence

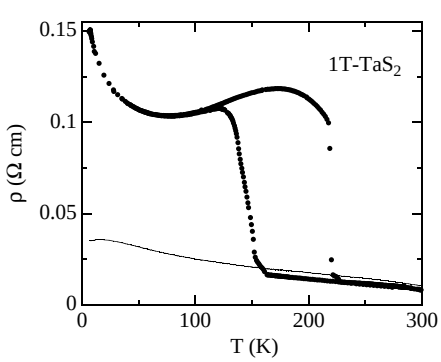

FIG. 1. In-plane resistivity of pure (solid symbols) and disordered $1T$-TaS_2 (line). The first order MI transition in the pure sample occurs at the NC-C transition, and presents a large hysteresis. The transition is completely suppressed in d-TaS_2.

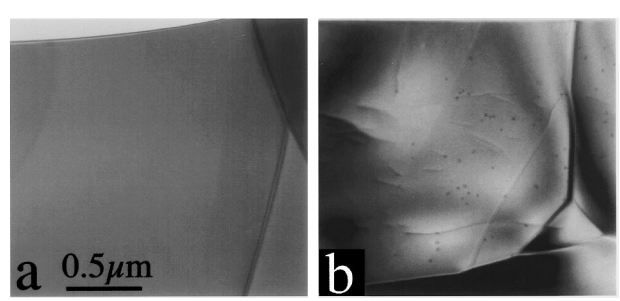

FIG. 2. Bright field TEM images of the pure (a) and disordered (b) samples of Fig. 1, showing a much denser dislocation network in the d-TaS_2 crystal.

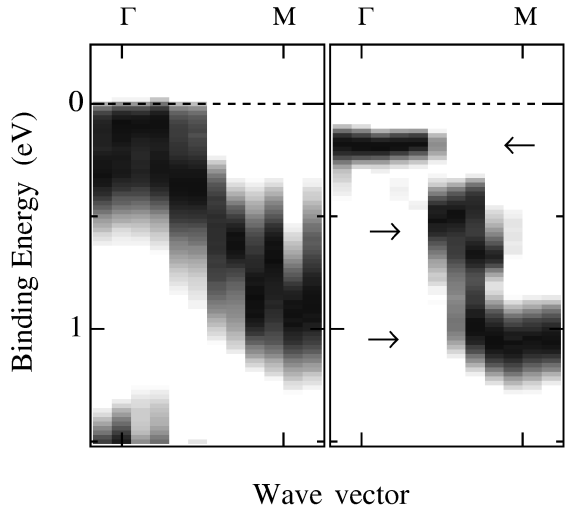

FIG. 3. ARPES intensity plots of $1T$-TaS_2 along the high symmetry ΓM direction. In the NC phase ($T = 250$ K, left) a single dispersing band of Ta d symmetry is observed. In the C phase ($T = 90$ K, right) the Ta d band splits into three subbands (marked by arrows), and a correlation gap opens around the Γ point.

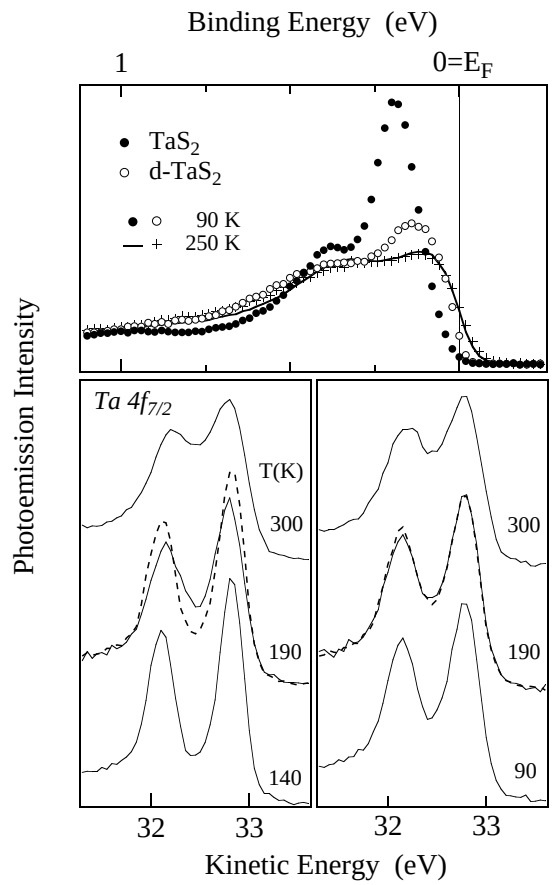

FIG. 4. Bottom: Temperature dependence of the Ta $4f_{7/2}$ core lines ($h\nu = 60$ eV) in pure (left) and disordered $1T$-TaS_2 (right). The line splitting reflects inequivalent Ta sites in the CDW state. The incomplete splitting indicates smaller domain sizes d-TaS_2. A Shirley background has been subtracted from the raw data. Top: High resolution valence band spectra ($h\nu = 20$ eV) of pure and d-TaS_2 at the Γ point.

band spectra of Fig. 4. Well into the NC phase, the line shapes of pure and d-TaS_2 are identical. There is emission at E_F, from the flat quasiparticle band seen in Fig. 3. However, the spectra of the two samples are considerably different at lower temperature. The spectrum of the pure sample is dominated by a sharp feature at 0.19 eV, associated with the lower Hubbard subband, and the intensity at E_F is extremely small, reflecting the correlation gap in the C phase [15]. The 90 K spectrum of d-TaS_2 is intermediate between the high- and the low-temperature spectra of TaS_2. The momentum dependence of the weak peak at 0.13 eV (not shown) follows that of the LHB of Fig. 3. The intensity at E_F is reduced from the high temperature spectrum, but only by $\sim$50%.

According to TF, the commensurate domains and the discommensurations play very different roles. Within the C domains, the d manifold splits under the influence of the CDW potential, favoring the opening of a correlation gap in the topmost subband. However, the transition cannot occur as long as free carriers, available from the domain boundaries, can sufficiently screen the electron-electron interaction within the narrow subband. The number of free carriers steadily decreases as the domains grow in the NC phase [3]. In the pure sample, possibly due to the increasing rigidity of the CDW and/or to the larger interplane coupling, the discommensurations are suddenly expelled from the sample at the lock-in transition. Screening is abruptly reduced, and the e-e Coulomb interaction strength U exceeds the critical value for the Mott-Hubbard transition [6]. The fingerprints of these temperature-dependent modifications have been directly observed in high-resolution ARPES experiments [14,15]. However, just from the spectra of pure TaS_2, it is impossible to disentangle the effects of long range CDW order and Coulomb interaction. A comparison with the disordered sample provides now this opportunity.

Defects, with their random pinning action, freeze the domain structure and prevent the incipient transition. The spectral properties of this frustrated state are intermediate between the high-temperature metal, and the correlated insulator. Free electrons available at the domain boundaries partially screen the e-e interaction, and the splitting of the topmost d-band is reduced. From the ARPES spectra we can determine quantitatively this effect. The binding energy of the ARPES peak is proportional to U, and probably close to $U/2$, since tunneling spectroscopy data show symmetric features around E_F [20]. For our disordered sample we obtain $U \sim 0.25$ eV, or only $\sim 2/3$ of U in the insulating phase. Because of the random distribution of defects, it is unlikely that all domains will have exactly the same size. The degree of commensuration and the strength of the screened Coulomb interaction will somewhat vary from domain to domain. Therefore, the U value obtained

from the ARPES spectrum should be considered as an average over a distribution of domain sizes. Nevertheless, the fact that the spectrum exhibits a sharp peak indicates a narrow distribution. Our data also allow us to exclude phase separation, i.e., the formation of insulating islands in a metallic matrix. In this case we would expect an incoherent superposition of spectra of the metallic and insulating phases. The observation of an intermediate spectrum, with a reduced peak energy, rules out this possibility. A quantitative analysis supports this conclusion.

Screening effects such as those presented here are not observed in the spectral function of typical Mott-Hubbard insulators, like the early transition metal oxydes [21]. In our opinion, this different behavior further confirms the peculiar nature of the MI transition and the importance of the CDW domain structure in $1T$-TaS_2. Clearly, the presence of free carriers from discommensurations plays a fundamental role. Long range CDW order, which eliminates this screening mechanism, must be achieved for the transition to take place. Moreover, even in the C phase, the insulating state is only marginally stable in $1T$-TaS_2 [16], and therefore easily disrupted by small changes in the strength of the interactions.

In summary, we investigated the spectral fingerprints of disorder and frustration of the MI transition in $1T$-TaS_2. Failure to establish a coherent CDW state, due to pinning, yields a $\sim 1/3$ reduction of the on-site Coulomb interaction, and strongly modifies the electronic states near the Fermi surface. These results provide an unusual and direct view of the evolution of the electronic structure of a 2D material under the effect of increasing correlations, from an incipient to a real Mott transition.

We gratefully acknowledge clarifying discussions with H. Mutka. One of us (M. G.) is indebted to F. Del Dongo for many stimulating suggestions. This work has been supported by the Swiss National Science Foundation and the Wisconsin Alumni Research Foundation. The Synchrotron Radiation Center, University of Wisconsin-Madison, is supported by NSF under Award No. DMR-95-31009.

[1] J. A. Wilson, F. J. DiSalvo, and S. Mahajan, Adv. Phys. **24**, 117 (1975).
[2] K. Nakanishi and H. Shiba, J. Phys. Soc. Jpn. **43**, 1839 (1977).
[3] X. L. Wu and C. M. Lieber, Phys. Rev. Lett. **64**, 1150 (1990).
[4] B. Burk, R. E. Thomson, A. Zettl, and J. Clarke, Phys. Rev. Lett. **66**, 3040 (1991).
[5] A. H. Thomson, F. R. Gamble, and J. F. Revelli, Solid State Commun. **9**, 981 (1971).
[6] P. Fazekas and E. Tosatti, Philos. Mag. B **39**, 229 (1979).
[7] F. J. Di Salvo, J. A. Wilson, B. G. Bagley, and J. V. Waszczak, Phys. Rev. B **12**, 220 (1975).
[8] H. Mutka, L. Zuppiroli, P. Molinié, and J. C. Bourgouin, Phys. Rev. B **23**, 5030 (1981).
[9] W. L. McMillan, Phys. Rev. B **12**, 1187 (1975).
[10] X. L. Wu, P. Zhou, and C. M. Lieber, Phys. Rev. Lett. **61**, 2604 (1988).
[11] H. Berger *et al.* (to be published).
[12] R. A. Pollak, D. Eastman, F. J. Himpsel, P. Heimann, and B. Reihl, Phys. Rev. B **24**, 7435 (1981).
[13] N. V. Smith, S. D. Kevan, and F. J. DiSalvo, J. Phys. C **18**, 3175 (1985).
[14] R Manzke, T. Buslaps, B. Pfalzgraf, M. Skibowski, and O. Anderson, Europhys. Lett. **8**, 195 (1989).
[15] B. Dardel *et al.*, Phys. Rev. B **45**, 1462 (1992); B. Dardel *et al.*, Phys. Rev. B **46**, 7407 (1992).
[16] A careful analysis of the spectra near E_F reveals that the tails of the lower and upper Hubbard bands have a very small but still finite (and temperature-dependent) overlap. The binding energy of the shallow flat band reflects the large energy scale set by the Coulomb correlation energy U, but the correlation gap is vanishingly small (very deep pseudogap) [15].
[17] H. P. Hughes and R. A. Pollak, Philos. Mag. **34**, 1025 (1976).
[18] G. K. Wertheim, F. J. DiSalvo, and S. Chiang, Phys. Rev. B **13**, 5476 (1976).
[19] H. P. Hughes and J. A. Scarfe, Phys. Rev. Lett. **74**, 3069 (1995).
[20] J. J. Kim, I. Ekvall, and H. Olin, Phys. Rev. B **54**, 2244 (1996).
[21] A. Fujimori *et al.*, Phys. Rev. Lett. **69**, 1796 (1992).